Impact of demagnetising fields on the magnetocaloric effect of gadolinium

Author: Quim Badosa Felip.
Facultat de Física, Universitat de Barcelona, Martí i Franquès 1, 08028 Barcelona, Spain.

Advisor: Enric Stern-Taulats

Abstract: Gadolinium is a benchmark magnetic refrigerant thanks to its near room temperature Curie point. In this study, the influence of demagnetising fields on the magnetocaloric response in gadolinium plates is quantified from direct measurements of magnetic field-driven adiabatic temperature changes ΔT_{ad}. Experimental data are analysed using the geometry-related demagnetising factors in the background of mean-field theory, and are correlated with the critical behaviour of $\Delta T_{ad}(H)$ at the Curie point. Results evidence that internal magnetic fields can be highly affected by sample orientation and differ significantly from the values of the applied magnetic fields. On the negative side, this translates to a reduction in the magnitude of the magnetocaloric properties that should always be quantified when these effects are enhanced in particular sample geometries. On the positive side, it is shown that demagnetising fields that are induced by the mechanical rotation of the sample at constant applied magnetic fields can be a viable driving force for the magnetocaloric effects, as illustrated by directly collected data of $\Delta T_{ad} = 0.9 \pm 0.1$ K for $\mu_0 \Delta H = 1.6$ T. These consequences are discussed in Brayton refrigeration cycles.

I. INTRODUCTION

Magnetocaloric effects rely on the thermal response of a given material to changes in an applied magnetic field [1]. When the field is applied isothermally, the caloric effect is measured by an entropy change (ΔS_m) related to the heat exchanged with the surroundings. When applied adiabatically, it is characterised by a temperature change (ΔT_{ad}). Based on these two changes, solid-state refrigeration cycles can be designed from magnetocaloric materials that could potentially replace the environmentally harmful refrigeration gases currently in use.

Gadolinium (Gd, Z=64) is a benchmark magnetocaloric material that shows a large magnetocaloric effect near its paramagnetic-ferromagnetic phase transition [2]. It is the only rare earth element that orders magnetically near room temperature ($T_C = 293K$) and is considered a simple Heisenberg ferromagnet. It has a large magnetic moment due to seven unpaired 4f electrons, which have a total angular momentum of $J = L + S = 7/2$.

The entropy and temperature changes are given by eqs.(1) and (2) [1], and they are expected to be enhanced near the phase transitions as the temperature derivative of the magnetisation (order parameter for this particular transition, M) is greatly enlarged.

$$\Delta T_{ad}\,(0 \to H') = -\int_0^{H'} \frac{T}{C_p}\left(\frac{\partial M}{\partial T}\right)_H dH \qquad (1)$$

$$\Delta S_m\,(0 \to H') = \int_0^{H'} \left(\frac{\partial M}{\partial T}\right)_H dH \qquad (2)$$

Where H is the magnetic field applied and C_p the heat capacity.

The magnetisation is maximised because the forces that tend to align the magnetic moments of the electrons in the material (ordering force) and the forces that tend to randomise them (disordering force) are in balance near T_C. Hence, the isothermal application of a magnetic field produces a much greater increase in magnetisation, i.e., an increase of the magnetic order and, consequently, a decrease in magnetic entropy near the Curie point, resulting in a large $\mid \Delta S_m \mid$. As the temperature increases above the Curie temperature, the thermal vibrations of the lattice become stronger, and the disordering force becomes dominant, leading to a decrease in the magnetisation. As the temperature decrease below T_C, the ordering force becomes dominant and the net magnetic field and magnetisation increase.

In this work we measured the adiabatic temperature changes while applying and removing magnetic field in two different positions: the z-axis of Gd plates parallel and perpendicular to the applied field. Experiments are carried out over the temperature interval [280, 320] K. Furthermore, temperature changes have been measured while changing these two positions with a constant field applied.

II. THEORETICAL BACKGROUND

The magnetisation M is defined as the magnetic moment per unit volume [3]. It is considered a continuous vector everywhere inside the material except at the edges, where it has to vanish. This results in a divergence of M leading to a divergence of magnetic field in the opposite direction known as the demagnetising field (H_d): $\nabla \cdot H_d = -\nabla \cdot M$. The situation is as if magnetic poles appear at the ends of the material creating H_d. When the poles are far from each other one can consider that they do not interact so the demagnetising field is zero. Figure 1 schematises this phenomenon for the case of a flat plate geometry. As a result the internal magnetic field (H_{int}) can be written in the general form

$$H_{int} = H_{app} + H_d \ , \qquad H_d = -N_z \cdot M \qquad (3)$$

where N_z is called demagnetising factor [4–6]. N_z is a function that depends on the shape of the sample with

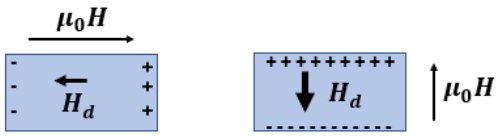

FIG. 1: Demagnetisation in a flat plate viewed in cross-section. Field applied through *Left:* the long axis, only a few magnetic poles are created, negligible H_d *Right:* the short axis, magnetic poles are created, large H_d.

respect to the applied field axis and ranges from 0 to 1. In order to measure the effect of the demagnetising field, the magnetisation on basis of the Weiss ferromagnetic molecular mean field model [7] is computed.

$$M = NgJ\mu_B \mathcal{B}_J \left(\frac{Jg\mu_B}{k_B} \frac{H + \lambda(M)M}{T} \right) \tag{4}$$

where N is the density of magnetic dipoles [8], g the g-factor [8], μ_B the Bohr magneton, B_J is the Brillouin function for spin J [9], k_B is the Boltzmann constant, H applied magnetic field, T the temperature, and λ the Weiss molecular mean-field exchange parameter [9]. From eq.4 it can readily be obtained that:

$$\frac{H}{M} = \frac{T - T_C}{C} + \frac{A_2}{C^2} T \cdot M^2 + \frac{A_3}{C^3} T \cdot M^4 + \dots \tag{5}$$

Where C is the Curie constant and A_2 and A_3 are constant factors [7]. By integrating eq.5 on M, the Gibbs free energy of the system is obtained as

$$G = G_0 + \frac{T - T_C}{2C} \cdot M^2 + \frac{A_2}{4C^2} T \cdot M^4 + \dots - H \cdot M \tag{6}$$

$$\left(\frac{\partial G}{\partial M} \right)_{M=M_{eq}} = 0 \quad ; \quad S = -\left(\frac{\partial G}{\partial T} \right)_{M=M_{eq}} \tag{7}$$

Using the above relations, where M_{eq} is the equilibrium magnetisation, the field-dependence of magnetisation at $T \to T_C$ is given by

$$M = \left(\frac{C^2}{K} \right)^{\frac{1}{3}} \left(\frac{H}{C} \right)^{\frac{1}{3}} + \dots \tag{8}$$

Where K is a constant [7]. Then, the magnetic field induced entropy change is

$$-\Delta S_m = \frac{1}{2C} \left(\frac{C^2}{K} \right)^{2/3} \left(\frac{H}{T_C} \right)^{2/3} + \dots \tag{9}$$

Since $-\Delta S_m \propto \Delta T_{ad}$ at $T = T_C$ [10], Mean Field Theories predict that near T_C, the adiabatic temperature change ΔT_{ad} scales with magnetic field as $H^{2/3}$.

III. EXPERIMENTAL DETAILS

Figure 2 shows the experimental setup used during the experiment. Magnetic field is applied by means of an

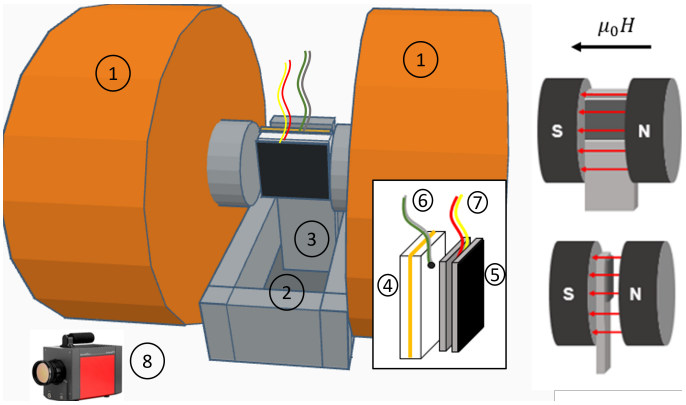

FIG. 2: *Left*:Experimental Device. **(1)** Magnet coils, **(2)** Thermal bath, **(3)** Sample holder,**(4)** Peltier module, **(5)** Sample, **(6)(7)** Thermocouples, **(8)** IR camera. *Right:* Sample placement.

electromagnet (GMW Magnet Systems, 209). The applied field is measured by a calibrated Hall probe and controlled by a computer program which outputs the current that circulates through the two coils from a current amplifier. With the given sample dimensions, the system allows the application of magnetic fields up to 2 T at varying rates of 2 T s^{-1} and -1.1 T s^{-1}.

A 20x20 mm^2 Peltier module has been used for the temperature control of the sample in the range of 280-320 K by applying electric currents in the range of ± 4 A. A type K thermocouple has been used to monitor the temperature of the top face of the Peltier module and fine-tune its input current. The sample has been placed on top of this Peltier module's face while the bottom face is in contact with a heat sink consisting of an aluminium rod emerging from a thermal water bath. Conductive thermal paste has been used to improve thermal contact between the Peltier module and the aluminium rod. The Gd sample has been placed between the magnet poles and the Peltier module and has been insulated by polystyrene to improve adiabaticity for magnetocaloric measurements. The ensemble of the sample and the Peltier module allows rotation to vary the magnetic field incident angle with the sample. Figure 2 illustrates the parallel and perpendicular cases that have been studied. Gd samples are mounted in sandwich mode consisting of two sheets of 20 x 20 x 0.2 mm^3 dimensions and a thermocouple inserted between the two sheets. To minimise the thermal influence of the thermometer on the temperature measurement, a fast-response fine-gauge type K thermocouple of 0.076 mm conductors diameter is used, which allows data acquisition at 5 Hz. This double mounting of the sample has been established after analysing the heat transfer conditions in a set of three individual sheets with rectangular (6 x 20 x 0.2 mm^3), square (20 x 20 x 0.2 mm^3), and needle (1.5 x 20 x 0.2 mm^3) geometries. Single sheet led to underestimating the magnetocaloric temperature changes due to deficient thermal contact and low active magnetocaloric mass surrounding the thermocouple.

For infrared (IR) temperature measurements, the outer surface of the sample has been painted with a thin layer of black paint (Lab IR Paint) to enhance its light emissivity. An IR camera (Infratech Image, IR 8800) has been used for IR imaging, allowing high-resolution spatial definition and high-frequency data acquisition up to 100 Hz. The temperature of the ensemble was smoothly changed from 280 to 320 K at 0.02 K s^{-1} while rapidly applying and removing magnetic fields in two different positions: the z-axis of the sample parallel and perpendicular to the applied field (Figure 4 right). Room temperature sample behaviour when changing these two positions with a constant field applied has been measured. Heat capacity data within the temperature range [250, 330] K has been obtained by MDSC measurements using a TA Q2000 calorimetre.

IV. RESULTS AND DISCUSSION

Figure 3 shows thermometry data collected during a heating run on magnetic field cycling. Each cycle is split into four parts: (1) adiabatic heating, (2) first thermalisation , (3) adiabatic cooling and (4) second thermalisation. The difference between the two thermalisation temperatures is because the field is varied before the sample reaches the environment temperature.

When measuring the temperature with the thermocouple spurious peaks appear when the field is applied and removed. These peaks are artefacts from induced voltages on thermocouple wires during fast variations of the magnetic field. Their effect can be overcome by linear extrapolation of data after 2 seconds, which corresponds to the magnetic field stabilisation time. Figure 3 also presents a section of this temperature sweep for the case of 1.6 T. There is a shift between the temperature measured by the IR and the thermocouple that, on one hand, can be attributed to slight calibration divergences and, on the other, environment reflections or heat waves measured by the camera. This could be improved by better isolating the measurement region.

Figure 4 shows the temperature change as a function of the sample temperature and the applied field in the parallel (left) and perpendicular (right) cases. Positive ΔT_{ad} values are obtained when the field is applied and negative ones when the field is removed. The magnitude of ΔT_{ad} is similar in both cases due to the high reversibility of the process. For the parallel case, the results obtained from the IR camera for selected values of the applied field are also plotted. It can be seen that the behaviour of ΔT_{ad} is similar to the thermocouple study. In other words, IR data on parallel mounting confirms the accuracy of thermocouple data and validate results obtained on perpendicular mounting. For this reason, in what follows, results have focused on the temperature changes obtained with the fine-gauge thermocouple, which can be measured in the two mounting configurations.

Perpendicular mounting allows for bringing the poles closer and larger magnetic fields up to 1.95 T. At the same time, the values of ΔT_{ad} obtained for 0.1 and 0.2

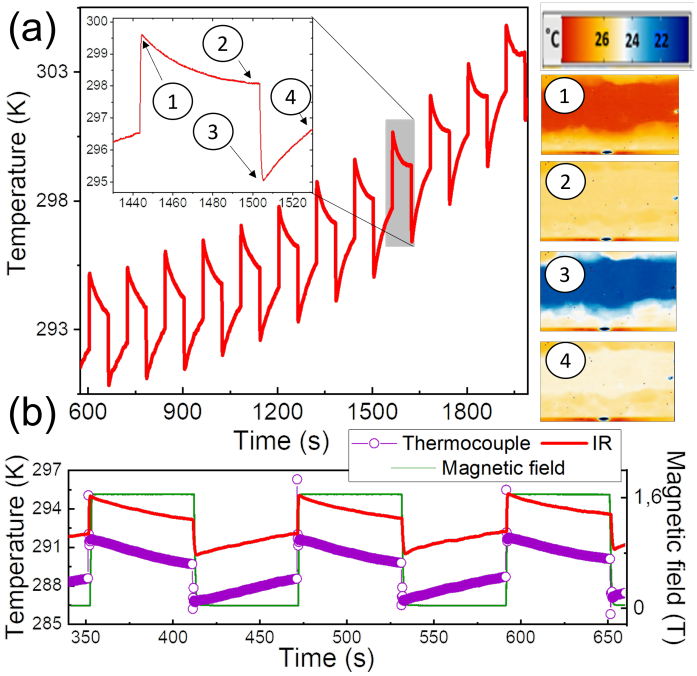

FIG. 3: **(a)** Graphic IR temperature behaviour when the sample is heated at 0.02 K s^{-1} when a magnetic field of 1.6 T is applied and removed. IR images at representative instants (see left inset) of one of the cycles. **(b)** Detail of the data collected with the fine-gauge thermocouple and Infrared Imaging when 1.6 T are cycled.

T applied are negligible. The maximum temperature change is near the Curie temperature.

Figure 5 shows the magnetic field dependence of ΔT_{ad} as a function of the magnetic field at the Curie temperature. It can be seen how the adiabatic heating and cooling values are generally coincident for both positions, which is indicative of the reversibility of the magnetocaloric effect in gadolinium. In addition, ΔT_{ad} values are systematically smaller when the magnetic field is applied perpendicular to the sample. The main difference between them comes from the effect that the demagnetising field has on the internal magnetic field in each situation and will be studied in the following section. Using the adiabatic parallel heating values to fit the MFT power-law approximation, $\Delta T_{ad} = (2.4 \pm 0.5) \cdot (\mu_0 H)^{(0.82 \pm 0.15)}$ is obtained. As explained above, the exponent $\alpha = 2/3$ is predicted from MFT [10, 11], which fits within the discrepancy range of our results ($\alpha = 0.82 \pm 0.15$). Comparing these results with the literature, Pecharsky and Gschneidner [2] find the relation $\Delta T_{ad} = 3.675 \cdot (\mu_0 H)^{0.7}$ while Bahl and Nielsen [12],$\Delta T_{ad} = 2.85 \cdot (\mu_0 H)^{0.78}$. Thus the exponent found here is close to the ones found in both articles but the prefactor is slightly lower.

A. Demagnetising field effect

In this section, the effect of the demagnetising field on the position of the samples is analysed. Two different cases to calculate the demagnetising factor [4] are

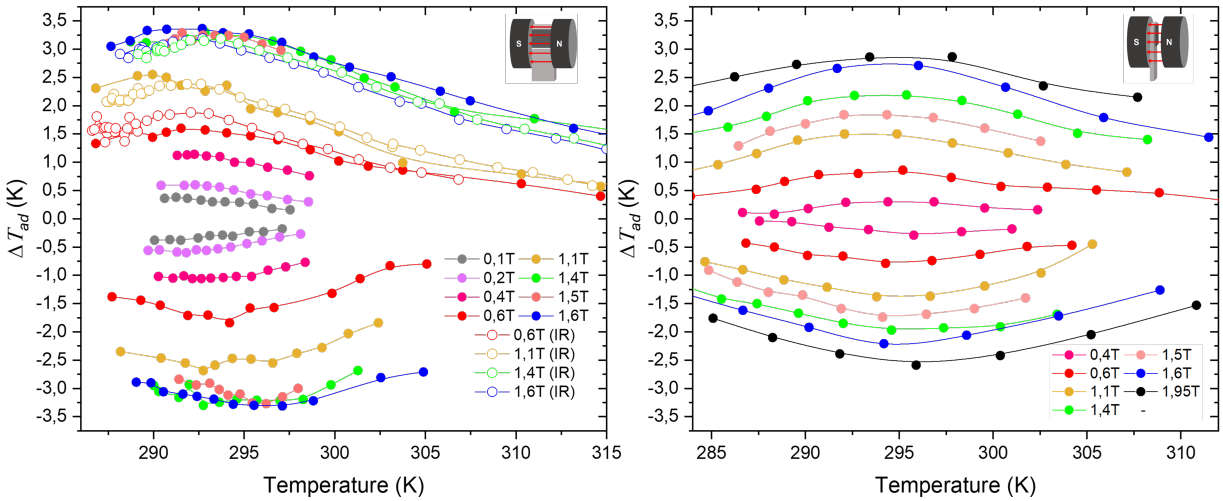

FIG. 4: Adiabatic temperature change for parallel (*left*) and perpendicular (*right*) orientations for different applied magnetic fields and temperatures. Solid symbols represent the results obtained with the thermocouple. Open symbols represent IR results for selected fields in the parallel position plot.

TABLE I: Demagnetising field effect for two different thicknesses: One sheet (1S) and two sheets (2S).

$\mu_0 H_{app}$ (T)		0.6	1.1	1.4	1.5	1.6	1.95
$\mu_0 H_d^{\perp}$ (T)	**1S**	0.479	0.584	0.642	0.651	0.661	0.719
	2S	0.464	0.566	0.622	0.631	0.640	0.696

considered: the first one where the thickness of the sample corresponds to the thickness of one sheet, and the second one where it corresponds to the thickness of two sheets that form the sandwich. The results are the following, **1 sheet:** $N_{Z\parallel} = 0.020$, $N_{Z\perp} = 0.958$. **2 sheets:** $N_{Z\parallel} = 0.035$, $N_{Z\perp} = 0.928$.

As expected, the perpendicular demagnetising factor gives a value close to 1, leading to a higher demagnetising field effect. For the parallel case N_z is close to 0, so the impact of H_d in the parallel position is considered negligible. Using eq.8, the effect on the internal magnetic field can be obtained. Table I shows the results obtained for the perpendicular case in terms of the applied field at T_C, results are similar when one or two sheets are used.

Figure 5 (right panel) includes ΔT_{ad} values for the perpendicular case when the magnetic field is corrected from the demagnetising factor. It is seen that all the data (perpendicular and parallel) collapse on a single curve which is consistent with the predictions of MFT.

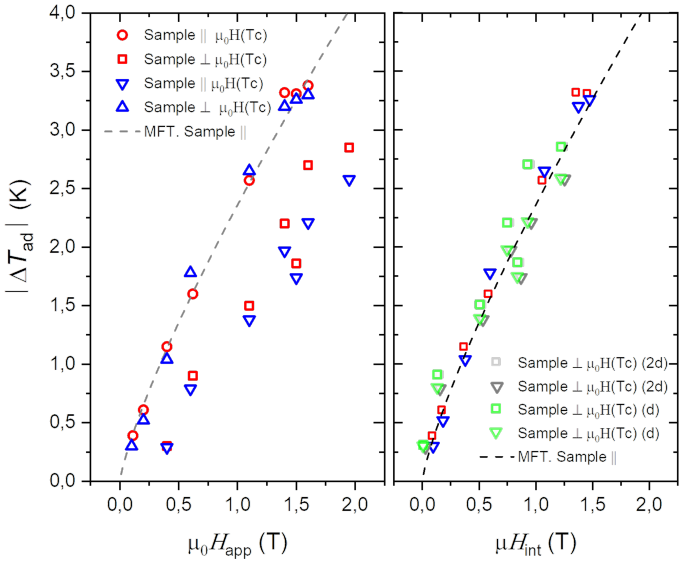

FIG. 5: *Left:*Absolute value of the adiabatic temperature change in terms of the applied magnetic field for both positions. Adiabatic heating and cooling are represented by *red* and *blue* symbols respectively. *Right:* Correction of the demagnetising field effect for the perpendicular case considering one (*green*) and two (*grey*) sheets.

B. Entropy

The entropy curve in the absence of magnetic field is obtained from C_p as $S - S_{ref} = \int_{T_{ref}}^{T'} \frac{C_p}{T} \delta T$, where T_{ref} is a reference temperature below the region of interest. From the entropy curve at zero field and the measured ΔT_{ad}, the entropy at a given field is readily obtained as illustrated in the panel (a) of Figure 6. It shows the entropy at 0 applied field and at 1.6 T in the parallel and perpendicular positions. Three possible magnetic Brayton cooling cycles sharing the same initial temperature are also plotted and magnified in the top left inset.

First, the field is applied adiabatically ($\Delta T_{ad} > 0$) and then the sample is allowed to cool following the isofield curve ($Q > 0$) back to the initial temperature. When the field is removed adiabatically the sample cools down. At zero field, the sample absorbs heat from the environment ($Q < 0$) and returns to the initial temperature.

The refrigerant capacity of a thermodynamic cycle (RC) is given by the enclosed area on the $S(T)$ diagram and determines the heat that can be extracted in a cooling cycle. If the parallel (C_1) and perpendicular (C_2) cycles shown in Figure 6 are compared, it can be noticed

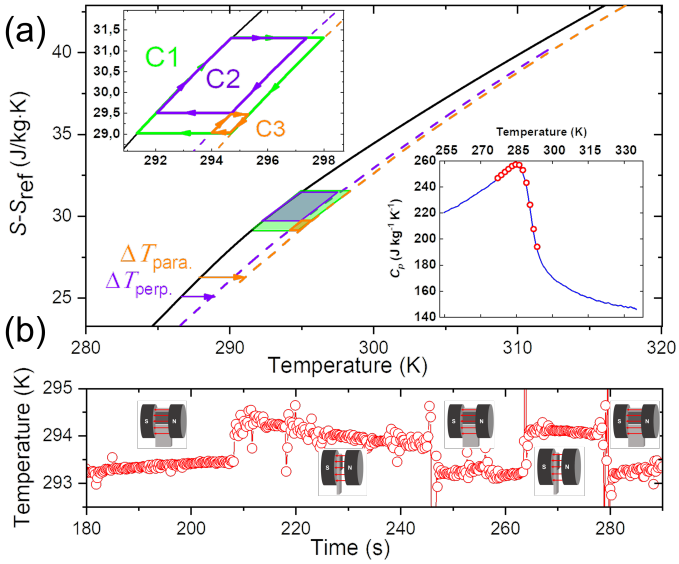

FIG. 6: **(a)**Entropy curves: No field (*black*) and 1.6T applied in parallel (*orange*) and perpendicular (*purple*) position. *Top left inset:* Three magnetocaloric Brayton refrigeration cycles. *Bottom right inset:* Heat capacity obtained from MDSC measurements. **(b)** Temperature data on the mechanical changes of the sample position at a constant applied magnetic field of 1.6T .

that the perpendicular case loses cooling power with respect to the parallel one.

For the cycle in which the sample is mounted parallel to the applied magnetic field ($C1$, green loop), $RC = 7.7$ J kg^{-1}.In contrast, when the sample is mounted perpendicularly to the applied field ($C2$, purple loop), the refrigeration cycle accounts for an $RC = 4.7$ J kg^{-1} , thus losing 38% of the cooling power due to lower internal magnetic fields and inefficient mounting.

It can also be seen that there is a possible refrigeration cycle created by changing the position of the sample (C_3). The possibility of such a cycle has been confirmed by applying a constant field of 1.6 T and rotating the sample between the two positions as quickly and stably as possible. A temperature difference is observed when moving from the perpendicular to the parallel position (Figure 6 (b)) due to the change in the internal magnetic field. In the case studied this value is $\Delta T_{ad} = 0.9 \pm 0.1$ K.

V. CONCLUSIONS

Magnetocaloric effect using both IR imaging and fine-gauge thermocouples has been characterised in gadolinium samples. The reversibility of the process when applying and removing magnetic field has been verified. ΔT_{ad} results obtained are consistent with the literature and follow the behaviour predicted by MFT. Moreover, the influence of the demagnetising field on the magnetocaloric effect has been analysed and corrected by comparing parallel and perpendicular mounting. Based on this effect, the behaviour of the temperature change has been studied and directly determined when the sample is rotated at constant field, giving as a result $\Delta T_{ad} = 0.9 \pm 0.1$ K when constant magnetic fields of 1.6T are applied. This result suggests that demagnetising fields not only have to be considered for the efficiency of the magnetocaloric effect but can also be its driving force.

Acknowledgments

I would like to thank Dr. Enric Stern-Taulats for his guidance, patience and dedication and for transmitting his knowledge and passion to me. I would also like to extend my gratitude to the research group for their help and to my family and friends who have supported me during this work.

[1] E. Stern-Taulats. *Giant caloric effects in the vicinity of first-order phase transitions*. PhD Thesis. Universitat de Barcelona (2017).

[2] A. M. Tishin, K.A. Gschneider Jr., S. Y. Dan'kov and V. K. Pecharsky. *Magnetic phase transitions and the magnetothermal properties of gadolinium*. Phys. Rev.**57**, 6 (1998).

[3] S. Blundell. *Magnetism in Condensed Matter*, Oxford University press, Oxford 2001, 1rst. ed.

[4] A. Aharoni. *Demagnetizing factors for rectangular ferromagnetic prisms*. J. Appl. Phys. **83**,6 (1998).

[5] D.X. Chen, E. Pardo and A. Sanchez. *Demagnetizing Factors for Rectangular Prisms*. IEE Transitions on Magnetics, **41**, 6 (2005).

[6] R.I. Joseph and E. Schlömann. *Demagnetizing Field in Nonellipsoidal Bodies*. J. Appl. Phys. **36**, 1579 (1965).

[7] J. H. Belo, J. S. Amaral, A. M. Pereira, V. S. Amaral and J. P. Araújo. *On the Curie temperature dependency of the magnetocaloric effect*. Appl. Phys. Lett. **100**, 242407 (2012).

[8] A. Smith, K. K. Nielsen, D. V. Christensen, C. R. H. Bahl, R. Bjørk and J. Hattel. *The demagnetizing field of a nonuniform rectangular prism*. J. Appl. Phys. **107**,103910 (2010).

[9] A. Planes. *Fenòmens Col·lectius i Transicions de Fase*. Universitat de Barcelona (2022).

[10] H. Oesterreicher and F. T. Parker. *Magnetic cooling near Curie temperatures above 300 K*. J. Appl. Phys. **55** , 4334 (1984).

[11] T. Gottschall, M. D. Kuz'min, K. P. Skokov, Y. Skourski, M. Fries, O. Gutfleisch, M. Ghorbani Zavareh, D. L. Schlagel, Y. Mudryk, V. Pecharsky and J. Wosnitza. *Magnetocaloric effect of gadolinium in high magnetic fields*. Phys. Rev. **99**, 134429 (2019).

[12] C. R. H. Bahl and K. K. Nielsen. *The effect of demagnetization on the magnetocaloric properties of gadolinium*. J. Appl. Phys. **105** , 013916 (2009).